

# IMPLICATIONS OF THE UPGRADE II OF LHCb ON THE LHC INSERTION REGION 8: FROM ENERGY DEPOSITION STUDIES TO MITIGATION STRATEGIES

A. Ciccotelli<sup>1\*</sup>, F. Cerutti, F. Butin, L. S. Esposito, B. Humann<sup>2</sup>  
M. Wehrle, CERN, Geneva, Switzerland  
R. B. Appleby, University of Manchester, Manchester, United Kingdom  
<sup>1</sup>also at University of Manchester, Manchester, United Kingdom  
<sup>2</sup>also at Wien University of Technology, Vienna, Austria

## Abstract

Starting from LHC Run 3, a first upgrade of the LHCb experiment (Upgrade I) will enable operation with a significantly increased instantaneous luminosity in the LHC Insertion Region 8 (IR8), up to  $2 \cdot 10^{33} \text{ cm}^{-2} \text{ s}^{-1}$ . Moreover, the proposed second upgrade of the LHCb experiment (Upgrade II) aims at increasing it by an extra factor 7.5 (up to  $1.5 \cdot 10^{34} \text{ cm}^{-2} \text{ s}^{-1}$ , as of Run 5) and collecting an integrated luminosity of  $400 \text{ fb}^{-1}$  by the end of Run 6. Such an ambitious goal poses challenges not only for the detector but also for the accelerator components. Monte Carlo simulations represent a valuable tool to predict the implications of the radiation impact on the machine, especially for future operational scenarios. A detailed IR8 model implemented by means of the FLUKA code is presented in this study. With such a model, we calculated the power density and dose distributions in the superconducting coils of the LHC final focusing quadrupoles (Q1-Q3) and separation dipole (D1) and we highlight a few critical issues calling for mitigation measures. Our study addresses also the recombination dipole (D2) and the suitability of the present TANB absorber, as well as the proton losses in the Dispersion Suppressor and their implications.

## INTRODUCTION

The High Luminosity LHC (HL-LHC) is meant to extend the physics discovery potential of the LHC experiments in the next two decades, reaching a proton-proton integrated luminosity of 3000 to  $4000 \text{ fb}^{-1}$  in the ATLAS and CMS detectors [1]. The LHCb experiment, placed in the Insertion Region 8 (IR8), was originally designed to operate at a lower luminosity ( $2 \cdot 10^{32} \text{ cm}^{-2} \text{ s}^{-1}$ ) with respect to the two general purpose LHC experiments and looks to explore complementary physics to ATLAS and CMS [2]. The LHCb detector is a single arm forward detector placed close to the vacuum chamber. The LHCb maximum luminosity was limited on purpose to guarantee the primary vertex detection. Recently, a first upgrade (LHCb Upgrade I) has been implemented during the Long Shutdown 2 (LS2 from December 2018 to mid-2022) enabling operation with a significantly increased instantaneous luminosity of up to  $2 \cdot 10^{33} \text{ cm}^{-2} \text{ s}^{-1}$ . Nevertheless, the Upgrade I does not fulfil the ultimate precision goals for many key observables, as described in [3], and

therefore, a second upgrade of the LHCb experiment (Upgrade II), proposed for installation in LS4, aims to reach a 7.5 times higher instantaneous luminosity ( $1.5 \cdot 10^{34} \text{ cm}^{-2} \text{ s}^{-1}$ ) to collect an integrated luminosity of  $400 \text{ fb}^{-1}$  by the end of the HL-LHC era. Such an ambitious goal poses challenges not only for the detector but also from the point of view of the sustainability and safety of the LHC. The key points are related to the absence of the protection elements installed instead in IR1 (ATLAS) and IR5 (CMS), and considered so far unnecessary in IR8 due to the lower peak luminosity, e.g. TAS and TAN absorbers and TCL collimators [4]. The objective of this study is to provide an overview of the main challenges associated to the Upgrade II, concerning the potential radiation induced degradation of LHC magnets, the possibility to operate the superconducting ones without recurrent occurrence of quenches (i.e. transition to the normal conducting state due to radiation heat), and the increased heat load on the cryogenic system. Consequent mitigation measures are introduced.

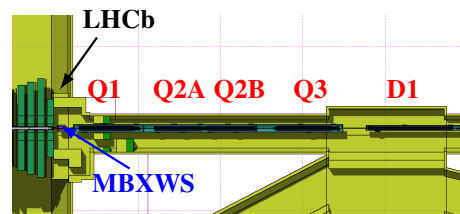


Figure 1: 3D top view of the FLUKA geometry including the muon detector of the LHCb detector (on the left) and the LHC final focusing triplet quadrupoles (Q1-Q2A-Q2B-Q3) and separation dipole (D1). The short warm dipole compensator (MBXWS) is also indicated.

## THE FLUKA MODEL OF IR8

A detailed IR8 model implemented by means of the FLUKA code [5–7] is used in this study. The accelerator section has been assembled using a dedicated Python-based tool, called Linebuilder [8]. In addition to the lattice elements, the model of IR8 features the detector, the experimental cavern and the LHC tunnel, including service tunnels and alcoves. Figure 1 shows the geometry layout on the right side of the Interaction Point 8 (IP8). The presence of the LHCb dipole produces a deflection of the circulating beam on the horizontal plane. This magnet is designed to operate with two

\* alessia.ciccotelli@cern.ch

opposite polarities, in order to collect the same integrated luminosity for either configuration. Its kick is compensated by three warm dipoles: the MBXWH placed on the left side of IP8 and two shorter magnets (MBXWS) in front of either final focusing triplet. The FLUKA model extends downstream towards the separation dipole (D1), where there is the transition from a single pipe to two separate vacuum chambers. The first element embracing both pipes is the TANB absorber, recently installed to protect the recombination dipole (D2) from the luminosity increase planned for Run 3. Moreover, the geometry covers the matching section (MS) and the dispersion suppressor (DS). The simulation parameters used for this study are reported in Table 1. The radiation shower across IR8 originates from proton–proton inelastic nuclear interactions in IP8 (including diffractive events). External vertical crossing is desirable for the LHCb physics programme because of the symmetry between the two detector magnet polarities, which simplifies the treatment of systematic uncertainties [9].

Table 1: Simulation Parameters Used for the FLUKA Simulation Studies After the Upgrade II [9]

<b>p-p collisions</b> $\sqrt{s}$	14 TeV
<b>Non-elastic cross section</b>	80 mb
<b>Ext. half crossing angle</b>	200 rad in vertical plane
<b>Integrated luminosity</b>	Final target 400 fb <sup>-1</sup>
<b>Instantaneous luminosity</b>	$1.5 \cdot 10^{34} \text{ cm}^{-2} \text{ s}^{-1}$

## FINAL FOCUSING QUADRUPOLES

The superconducting magnets of the final focusing triplet are particularly exposed to the collision debris. In the ATLAS and CMS insertions, the closest quadrupole to the IP (Q1) required a front absorber (called TAS) already at the design luminosity of  $10^{34} \text{ cm}^{-2} \text{ s}^{-1}$ . Our new IR8 results are shown in Fig. 2 and indicate that, as expected, on the IP side of the Q1 the peak power density in the inner superconducting coils exceeds the quench limit<sup>1</sup> of 13 mW/cm<sup>3</sup> [10].

Furthermore, the calculation of the respective dose after 400 fb<sup>-1</sup>, assuming that half of the integrated luminosity is collected with either polarity of the LHCb spectrometer, yields a maximum of about 50 MGy, well above the estimated quadrupole damage limit of 30 MGy [11]. As a consequence, a protection strategy is necessary both to avoid the quench risk and reach the desired integrated luminosity target. The proposed solution [4] is the integration of an absorbing material inside the yoke of the MBXWS, around the beam pipe (with the resulting element denominated as MBXWS-TAS). The simulation of the MBXWS-TAS, embedding a tungsten shield, provides a reduction of more than a factor two (see Fig. 3), down to a level already safely exceeded during the Run 2 operation at  $2 \cdot 10^{34} \text{ cm}^{-2} \text{ s}^{-1}$  in ATLAS and CMS.

<sup>1</sup> A value three times lower was taken as LHC design limit.

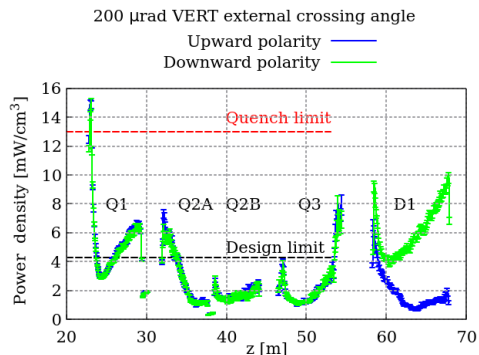


Figure 2: Longitudinal profiles of peak power density in the superconducting coils along the triplet and the D1 on the right side of IP8 (at  $z=0$ ). Values are averaged over the cable radial thickness with a 2° azimuthal resolution and normalized to  $1.5 \cdot 10^{34} \text{ cm}^{-2} \text{ s}^{-1}$ .

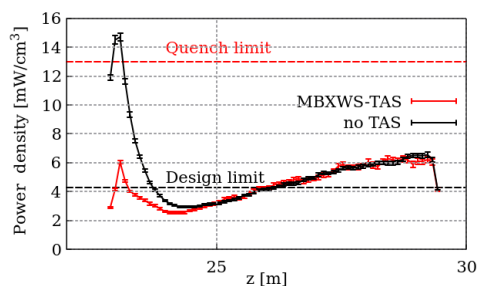


Figure 3: Longitudinal profiles of peak power density in the Q1 superconducting coils on the right side of IP8 (at  $z=0$ ), as in Fig. 2 (in black) and with the MBXWS-TAS tungsten shield (in red). Only the case of downward polarity of the LHCb spectrometer is shown, but the same effect is achieved for upward polarity.

The total power absorbed by the Q1 on the right side of IP8, which is more impacted than the one on the left (due to the geometry asymmetry), decreases from 220 W to 183 W, if one assumes that the shield extends up to a distance of 5 cm from the vacuum chamber center on either side in the horizontal plane. The global heat load requires a major upgrade of the cryogenic system that is presently limited to handle about 50 W for the whole triplet-D1 string.

## SHORT WARM COMPENSATORS

Despite its larger distance from IP8, the short warm compensator MBXWS is more exposed to radiation induced degradation than the long compensator, since it is impacted by more energetic forward angle particles. In particular, the coils above and below the vacuum chamber, on the IP face of the magnet, may be subject to accumulated dose values that overcome the insulator resistance. The simulated peak dose almost reaches 140 MGy after 400 fb<sup>-1</sup> (see Fig. 4), possibly causing a failure of the warm dipole [12]. In order to prevent it, the installation of a tungsten absorber on the vacuum chamber in front of the coils can be effective. Figure 4 indicates that a longitudinal thickness of 7-8 cm

could be sufficient to preserve the magnet functionality until achieving the final integrated luminosity target.

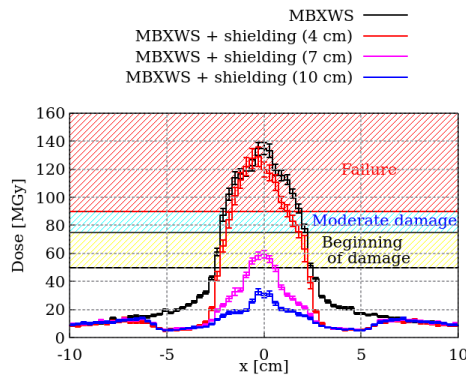


Figure 4: Transverse dose distribution in the upper coil on the IP face of the MBXWS.1R8 after  $400 \text{ fb}^{-1}$ , considering the addition of protective tungsten pieces of different thickness. The colored areas represent the damage ranges as described in [12].

## SEPARATION DIPOLE - D1

In Fig. 2, a second weak point is identified as the superconducting D1, whose limits, with regard to both quench risk and coil insulator damage, remain to be reviewed. In particular, the LHCb downward polarity configuration features challenging maxima on both extremities of the dipole. Thanks to its larger coil aperture, it is in principle possible to replace the actual D1 beam screen with a smaller one, identical to the Q3 beam screen, and this way leave room for increasing the thickness of the cold bore wall. Figure 5

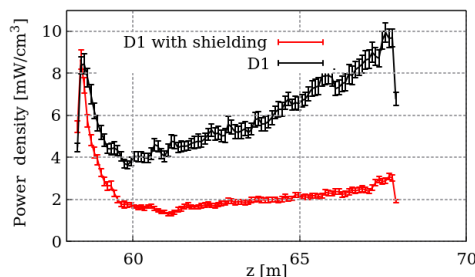


Figure 5: Longitudinal profile of peak power density in the D1 superconducting coils on the right side of IP8 (at  $z=0$ ) for LHCb downward polarity, as in Fig. 2 (in black) and with a 5.5 mm thicker cold bore stainless steel wall (in red).

shows that such a measure can remove the problem on the non-IP side. In order to substantially reduce the IP side peak, the upstream prolongation of the thicker beam tube shall be considered.

## RECOMBINATION DIPOLE - D2

As earlier mentioned, the new TANB absorber has been already installed to protect the D2 recombination dipole from the neutral component of the collision debris, in view of the

Run 3 luminosity increase. Our simulation results show that its protection role is fulfilled even for the Upgrade II luminosity targets, since it keeps the peak power density in the D2 superconducting coils below  $2 \text{ mW/cm}^3$  and the peak dose below 12 MGy. Nevertheless, the D2 total load is 50 W for the LHCb downward polarity, which is higher than the respective HL-LHC value in IR1 and IR5. Moreover, the TANB itself will need a cooling system to dissipate the absorbed power, which has been evaluated to be up to 150 W.

## MATCHING SECTION AND DISPERSION SUPPRESSOR

From preliminary studies carried out on the left side of IR8, the expected peak power density in the coils of the quadrupoles of the MS (Q4, Q5, Q6 and Q7) is below  $2 \text{ mW/cm}^3$  and peak dose values are less than 3 MGy. This puts in question the necessity of the TCL physics debris collimators. On the other hand, high energy proton losses in the DS impact the even half-cells, corresponding to the peaks of the optical dispersion function, with the largest power deposition taking place in the half-cell 8. Predicted levels are compatible with operational and lifetime limits of main dipoles and quadrupoles [10, 11], but require further investigations for corrector dipoles, whose radiation resistance is deemed to be significantly lower. In particular, the MCBC in half-cell 8 may call for the installation of one TCL collimator, to be placed at the end of the Long Straight Section (LSS).

## CONCLUSIONS

The proposed LHCb Upgrade II implies the design and implementation of mitigation measures on the accelerator side to cope with the desired luminosity increase. A TAS-MBXWS can effectively decrease the peak power density and dose in the Q1 coils to safe levels. For the protection of the MBXWS frontal coils, tungsten pieces of suitable length are necessary. The adoption of a thicker beam tube was proposed to reduce the expected radiation peak on the D1 non-IP extremity. It could be effective also for the other peak on the D1 IP side if prolonged upstream over a sufficient length. The TANB turns out to properly fit its D2 protection role also in the Upgrade II scenario. An upgrade of the cryogenic system is required for the final focusing triplet string and, to a lesser extent, for the recombination dipole. No evidence for the necessity of the TCL collimator scheme in IR8 was found, except for one element to be placed at the end of the LSS to protect the MCBC corrector in half-cell 8 from detrimental degradation.

## ACKNOWLEDGEMENTS

Research supported by the HL-LHC project. We would like to thank Riccardo De Maria, Francisco Sanchez Galan and Gerard Ferlin for useful discussions and analyses of our results, as well as the LHCb Collaboration for sharing the FLUKA model of the LHCb detector.

## REFERENCES

- [1] O. Aberle *et al.*, “High-Luminosity Large Hadron Collider (HL-LHC): Technical design report,” Tech. Rep., 2020, doi : 10.23731/CYRM-2020-0010
- [2] O. Brüning *et al.*, *LHC Design Report*. CERN, 2004, doi : 10.5170/CERN-2004-003-V-1
- [3] LHCb Collaboration, “Framework TDR for the LHCb Upgrade II - Opportunities in flavour physics, and beyond, in the HL-LHC era,” CERN, Tech. Rep., 2021, <https://cds.cern.ch/record/2776420>
- [4] I. Efthymiopoulos *et al.*, “LHCb Upgrades and operation at  $10^{34} \text{cm}^{-2} \text{s}^{-1}$  luminosity – A first study,” CERN, Tech. Rep. CERN-ACC-NOTE-2018-0038, 2018, <https://cds.cern.ch/record/2319258>
- [5] CERN, *Fluka website*, <https://fluka.cern>.
- [6] C. Ahdida *et al.*, “New Capabilities of the FLUKA Multi-Purpose Code,” *Frontiers in Physics*, vol. 9, 2022, doi : 10.3389/fphy.2021.788253
- [7] G. Battistoni *et al.*, “Overview of the FLUKA code.” *Ann. Nucl. Energy*, vol. 82, pp. 10–18, 2015, doi : 10.1016/j.anucene.2014.11.007
- [8] A. Mereghetti, V. Boccone, F. Cerutti, R. Versaci, and V. Vlachoudis, “The FLUKA LineBuilder and Element DataBase: Tools for Building Complex Models of Accelerator Beam Lines,” in *Proc. IPAC’12*, New Orleans, LA, USA, May 2012, pp. 2687–2689, <https://jacow.org/IPAC2012/papers/WEPPD071.pdf>
- [9] J. Albrecht *et al.*, “Luminosity scenarios for LHCb Upgrade II,” CERN, Tech. Rep. LHCb-PUB-2019-001, 2019, <https://cds.cern.ch/record/2653011>
- [10] N. V. Mokhov, I. L. Rakhno, J. S. Kerby, and J. B. Strait, “Protecting LHC IP1/IP5 Components Against Radiation Resulting from Colliding Beam Interactions,” CERN, Tech. Rep., 2003, <https://cds.cern.ch/record/613167>
- [11] M. Tavlet, A. Fontaine, and H. Schonbacher, “Compilation of radiation damage test data,” CERN, Tech. Rep. 98-01, 1998, <https://cds.cern.ch/record/357576/files/CERN-98-01.pdf>
- [12] P. Fessia and F. Cerutti, “Radiation levels of MBW and MQW,” CERN, Tech. Rep. 1952741 v.1, 2019.